Numerical Simulation of Gust Response of a One-DOF Wing in Stall Flutter

Xiaoyang Zhang*, Dominique Poirel†
Royal Military College of Canada, Kingston, Ontario, K7K 7B4, Canada

and Weixing Yuan‡
National Research Council Canada, Ottawa, Ontario, K1A 0R6, Canada

Abstract

This study presents numerical simulations of the gust response of a one-degree-of-freedom (one-DOF) wing in stall flutter. Prior to the gust loading, three-dimensional large-eddy simulations (3D LES) on the fluttering wing were conducted and validated against experimental results from the wind tunnel of the Royal Military College of Canada (RMC). After the validation, the transverse 'sine-squared' gust was introduced in the numerical simulation. The effects of gust width were also investigated.

I. Introduction

Gust effects can be particularly significant in urban areas, which is of interest for Urban Air Mobility applications. For instance, a transverse gust may dramatically alter the effective angles of attack (AOAs) of flight vehicles in urban environments, where the freestream velocity is relatively low. The large AOA may lead to stall flutter, which can be a critical consideration in the design of such vehicles. Thus, it is of interest to investigate the gust response of a wing in stall flutter for better understanding of the gust effects on aeroelasticity. Numerical simulations are conducted in this study to analyse the gust effects.

II. Numerical Results

A. Wing in Stall Flutter

In the RMC wind tunnel, stall flutter was investigated based on one-DOF pitch [1] and 2-DOF pitch-heave [2, 3] configurations. The experimental rig is shown in Fig. 1. A rigid but elastically mounted NACA 0012 wing with a chord of 0.156 m and a span of 0.61 m was studied. At two airspeeds, numerical simulations of a one-DOF wing in stall flutter were carried out by the National Research Council Canada (NRC) using the in-house CFD code INSflow with an implemented one-DOF structural model [1]. The O-type computational mesh is shown in Fig. 2. The mesh was dynamic based on the pitching motion.

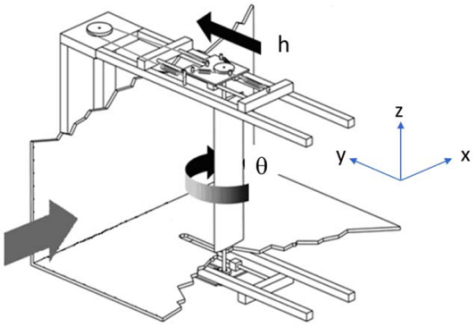

Fig. 1 Schematic of experimental setup at RMC, adopted from [3].

*Ph.D. Student, Department of Mechanical and Aerospace Engineering, xiaoyang.zhang@rmc-cmr.ca; visiting scholar at NRC, xiaoyang.zhang@nrc-cnrc.gc.ca.
†Professor, Department of Mechanical and Aerospace Engineering, poirel-d@rmc.ca.
‡Senior Research Officer, Aviation Aerodynamics, 1200 Montreal Road; weixing.yuan@nrc-cnrc.gc.ca.

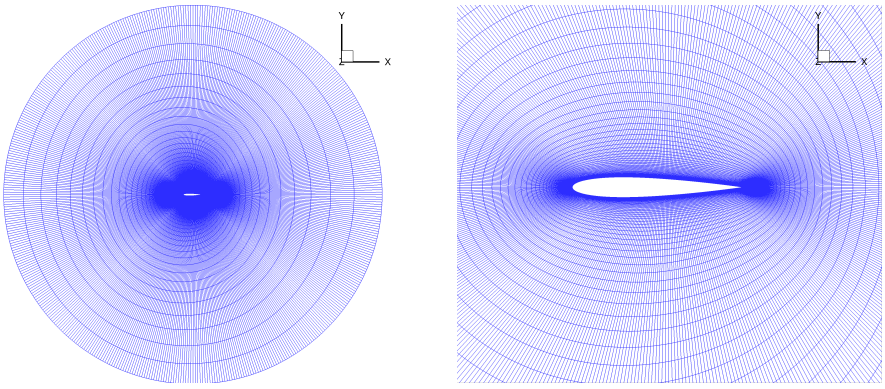

(a) (b)

Fig. 2 Illustration of the dynamic mesh: (a) 2D section of the 3D mesh; (b) close up on the wing.

Stall flutter simulations were further performed in this study and some results for a number of airspeeds are displayed in Fig. 3. Note that Re_c denotes Reynolds number based on airfoil chord length c and freestream velocity U_∞, $U_\infty c/\nu$. T corresponds to the experimentally-measured cycle period. From Fig. 3(a), it can be seen that the current numerical simulations predicted oscillation amplitude trend comparable to the experimental data, with over-predicted pitch amplitudes. This may be due to the non-captured 3D effects (aspect ratio of 0.2 for the CFD model; 3.9 for the experimental setup) or the imperfect structural parameters used for the simulation. According to the computed peak amplitude diagram along time of Fig. 3(b), it seems that with higher Re_c, the computed limit-cycle oscillations (LCOs) have more amplitude modulations. A revised CFD model with increased span length is being investigated and will be presented in a future publication.

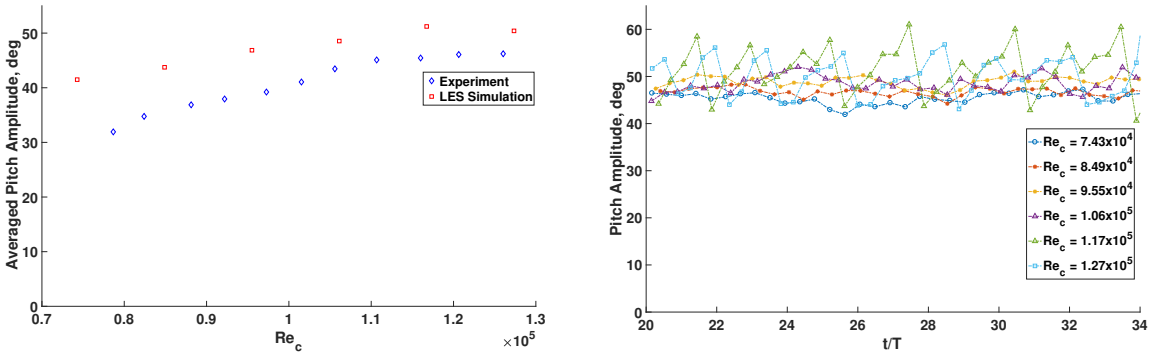

(a) (b)

Fig. 3 (a) Averaged peak amplitudes as a function of Re_c for experiments and 3D LES simulations; (b) Computed peak amplitudes of LCO along time for various Reynolds numbers.

B. Gust Response

Experimental investigations of small-amplitude and self-sustained aeroelastic oscillations of airfoils at low Reynolds numbers were conducted by Poirel et al. [4]. Yuan et al. [5] numerically captured the presence of the laminar-separation flutter with small-amplitude LCOs for a NACA 0012 airfoil under two DOFs at a transitional Reynolds number. To study the gust effects on the laminar-separation flutter, Yuan et al. [6] introduced transverse gusts with peak gust ratio ($GR = V_g/U_\infty = 0.16$) to the aforementioned numerical simulation. The detailed gust modelling can be found in [6]. It was shown that the gust had different effects on the post-gust LCOs, depending on the wing motion as it entered the gust. In this study, similar numerical simulations on gust responses are conducted for a one-DOF wing in stall flutter with large-amplitude oscillations, which is sketched in Fig. 4. Fig. 4 also defines the gust width (GW) of the 'sine-squared' gust.

Fig. 5 shows the spanwise vorticity ω_z on the cross-section at midspan of the wing in stall flutter in absence and presence of gusts at different instantaneous time for $U_\infty = 8$ m/s ($Re_c = 84{,}900$). For the gust loading case displayed

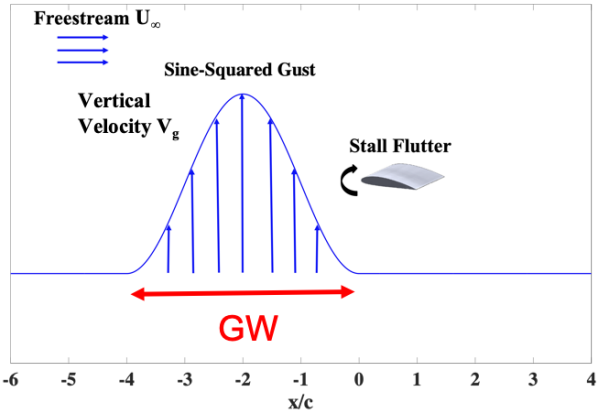

Fig. 4 Sketch of one-DOF wing in stall flutter encountering 'sine-squared' gust, GW = 4c.

by Figs. 5(d-f), the wing starts entering the gust, with GR = 0.2 and GW = 4c, at t/T = 1. The wing is located middle of the gust at t/T = 1.125, and leaves the gust completely at t/T = 1.25. The differences in the spanwise vorticity of the two configurations, with and without gusts, are apparent, which results in the change of aerodynamic loading and pitching motion of the wing. Regarding the pitch angles of the two scenarios, it is observed that they are close at t/T = 1 (approximately 1 deg difference), but the difference becomes noticeable when the 'touching' between the gust and wing ends. At t/T = 1.25, θ = -28 deg and -34 deg in absence and presence of gusts, respectively (see red and green lines at t/T = 1.25 when the wing leaves the gust completely in Fig. 6(a)).

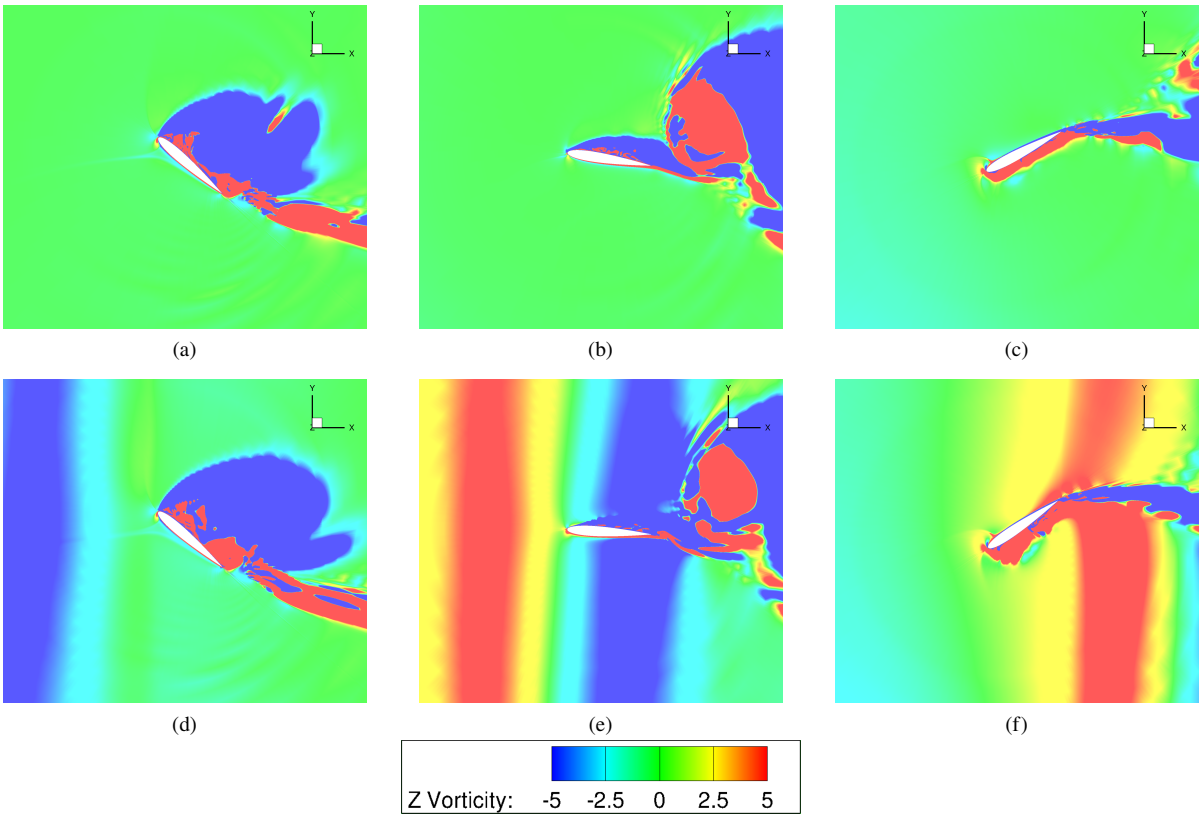

Fig. 5 3D LES-computed instantaneous spanwise vorticity ω_z distributions on the midspan of the one-DOF NACA 0012 wing in stall flutter without (top) and with (bottom) 'sine-squared' gust, GR = 0.2 and GW = 4c, at (a&d) t/T = 1; (b&e) t/T = 1.125; (c&f) t/T = 1.25 for U_∞ = 8 m/s, Re_c = 84,900.

The effects of GW on post-gust LCOs for two Reynolds numbers were also investigated. As seen from Fig. 6, gusts start affecting fluttering motion before the wing 'touches' the gust. With the same GR but larger GW, the gust effects are more significant for both airspeeds. In addition, the gusts affect not only the amplitude, but also the phase of the oscillations, especially for the larger airspeed. This phenomenon can also be seen from the different pitch angles of the wing in Figs. 5(c&f). Since stall flutter occurs due to the energy extraction of the oscillating wing coming from the airflow (dynamic stall effects), the physical mechanism of gust loading on dynamic stall effects is under investigation, which will be discussed in a future publication.

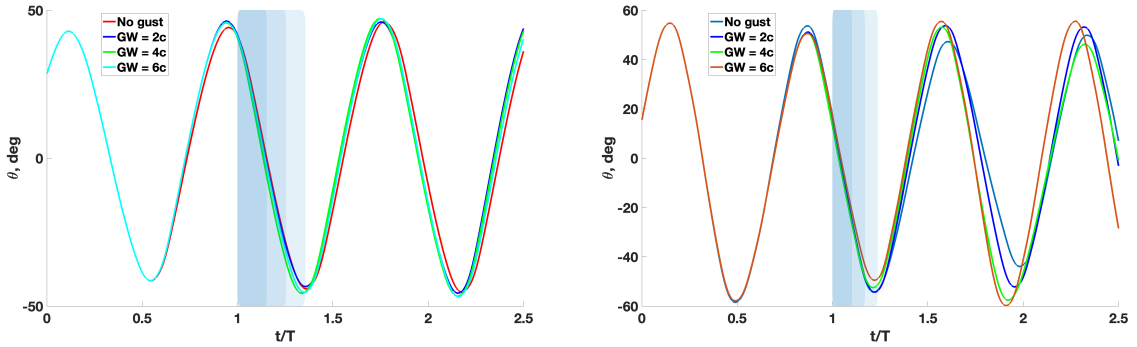

Fig. 6 3D LES computed pitching response of a NACA 0012 wing in stall flutter to 'sine-squared' gusts with different GW (wing entering gusts denoted by blue bands, lighter blue bands denoting larger GW, all starting at t/T = 1), GR = 0.2: (a) U = 8 m/s, Re_c = 84,900; (b) U = 12 m/s, Re_c = 127,000. Gusts are all activated at t/T = 0 except for no gust scenarios. θ denotes the pitch angle of airfoil.

III. Conclusion

The 3D LES-computed results predicted oscillation amplitude trend comparable to the experimental data, with over-predicted pitch amplitudes. The interaction between the fluttering wing and the gusts started in advance of the instantaneous time when the wing started entering the gusts. Moreover, larger gust width had more significant effects on both the oscillation amplitude and phase based on the current simulations.

Acknowledgments

The authors are very grateful to the financial support of the NRC Integrated Aerial Mobility (IAM) program and the funding from Natural Sciences and Engineering Research Council of Canada (NSERC).

References

[1] Goyaniuk, L., Poirel, D., Benaissa, A., and Yuan, W., "Analysis of One Degree-of-freedom Stall Flutter Limit Cycle Oscillations," *CASI AERO 2017*, Totonto, ON, May 16-18, 2017.

[2] Poirel, D., Goyaniuk, L., and Benaissa, A., "Frequency Lock-in in Pitch–heave Stall Flutter," *Journal of Fluids and Structures*, Vol. 79, 2018, pp. 14–25.

[3] Goyaniuk, L., Poirel, D., and Benaissa, A., "Pitch–heave Symmetric Stall Flutter of a NACA0012 at Transitional Reynolds Numbers," *AIAA Journal*, Vol. 58, No. 8, 2020, pp. 3286–3298.

[4] Poirel, D., Harris, Y., and Benaissa, A., "Self-sustained Aeroelastic Oscillations of a NACA0012 Airfoil at Low-to-moderate Reynolds Numbers," *Journal of Fluids and Structures*, Vol. 24, No. 5, 2008, pp. 700–719.

[5] Yuan, W., Poirel, D., and Wang, B., "Simulations of Pitch–heave Limit-cycle Oscillations at a Transitional Reynolds Number," *AIAA Journal*, Vol. 51, No. 7, 2013, pp. 1716–1732.

[6] Yuan, W., Zhang, X., and Poirel, D., "Numerical Modelling of Aerodynamic Response to Gust," *AIAA Scitech 2021 Forum*, 2021. https://doi.org/10.2514/6.2021-2001.